Computers and Concrete, *Vol. 19, No. 5 (2017) 467-475*
DOI: https://doi.org/10.12989/cac.2017.19.5.467

Prediction model of resistivity and compressive strength of waste LCD glass concrete

Chien-Chih Wang*

Department of Civil Engineering and Geomatics, Cheng Shiu University, 83347, Kaohsiung, Taiwan, R.O.C.

(Received September 12, 2015, Revised January 14, 2017, Accepted January 18, 2017)

Abstract. The purpose of this study is to establish a prediction model for the electrical resistivity (E_r) of self-consolidating concrete by using waste LCD (liquid crystal display) glass as part of the fine aggregate and then, to analyze the results obtained from a series of laboratory tests. A hyperbolic function is used to perform nonlinear multivariate regression analysis of the electrical resistivity prediction model, with parameters such as water-binder ratio (w/b), curing age (t) and waste glass content (G). Furthermore, the relationship of compressive strength and electrical resistivity of waste LCD glass concrete is also found by a logarithm function, while compressive strength is evaluated by the electrical resistivity of non-destructive testing (NDT). According to relative regression analysis, the electrical resistivity and compressive strength prediction models are developed, and the results show that a good agreement is obtained using the proposed prediction models. From the comparison between the predicted analysis values and test results, the MAPE value of electrical resistivity is 17.0-18.2% and less than 20%, the MAPE value of compressive strength evaluated by E_r is 5.9-10.6% and nearly less than 10%. Therefore, the prediction models established in this study have good predictive ability for electrical resistivity and compressive strength of waste LCD glass concrete. However, further study is needed in regard to applying the proposed prediction models to other ranges of mixture parameters.

Keywords: concrete; liquid crystal glasses; compressive strength; electrical resistivity; prediction model

1. Introduction

Manufactured LCD (liquid crystal display) panels are widely applied to information display devices used in life, such as in televisions, computer monitors, mobile phones and computers, personal digital assistants, navigation systems, and projectors. Since it was listed as the first-stage development priority of the "Two Trillion Core Industries Program", Taiwan's flat-panel display industry has flourished. In 2011, Taiwan's output accounted for 38% of the global large-size LCD panel production, thus, Taiwan has become one of the largest producers of LCD panels, second only to Korea. With the substantial increase in production, large amounts of waste are derived from the manufacturing process (Gao *et al.* 2008); hence, the proper disposal of waste LCD glass is an urgent issue.

The major materials of liquid crystal displays include glass (85-87%), polymer membrane (12.7-14%), and liquid crystal (0.12-0.14%) (Chang, 2005, Roland *et al.* 2004). Liquid crystal is composed of glass substrates, liquid crystal, ITO (indium tin oxide) conductive glass, and black matrix (chromium oxide), and is characterized as an interim state between a solid and a liquid (Wang *et al.* 2014c). The main chemical constituents of waste LCD glass are SiO_2, Na_2O, and a small amount of indium-tin-oxide conducting film. The conducting film is coated on the LCD to reduce the resistance of the substrate's surface, which enhances light transmittance and conductivity. Therefore, direct landfill, incineration, and composting treatments are inappropriate for waste LCD glass (Lin 2007). Glass is amorphous material with high silica content, and thus, is potentially pozzolanic when particle size is less than 75 μm (Sakale *et al.* 2016). Therefore, glass powder (GP) can be used as an alternative supplementary cementing material in concrete (Omran and Tagnit-Hamou 2016). Furthermore, the addition of crushed waste glass to concrete as a fine aggregate can effectively reduce the air content and unit weight of concrete, and improve its performance (Topcu and Canbaz 2004). In this study, the addition of waste LCD glass is used as part of the fine aggregate to replace natural sand. As waste LCD glass material can be reused, it can lead to a decrease in CO_2 emissions, rendering this recycling process the preferred method for sustainable development.

The inspection-based maintenance management framework, which is a particularly non-destructive testing (NDT) method, has been widely used to carry out inspections (Sheilsa *et al.* 2012); in particular, the strength assessment of existing buildings, which is a challenge for structural engineers who must feed structural computations with material data. Such assessment is required under various conditions: (a) when some damage has developed over time, (b) when new requirements must be addressed due to changes in regulations or the loads to be supported, (c) when the material's condition must be checked due to some suspicion, e.g., when the concrete in the control cast cylinders may differ from the concrete in the building itself.

*Corresponding author, Associate Professor
E-mail: ccw@gcloud.csu.edu.tw

http://www.techno-press.org/?journal=cac&subpage=8
ISSN: 1598-8198 (Print), 1598-818X (Online)

In any case, NDT techniques offer an interesting approach (Breysse 2012). The methods of ultrasonic pulse velocity and electrical resistivity of non-destructive testing have been widely applied to the investigation of mechanical properties and the integrity of concrete structures (Ramezanianpour *et al.* 2011, Shariq *et al.* 2013, Solis-Carcano and Moreno 2008, Vipulanandan and Garas 2008).

Previous studies generally focused on investigating the workability and strength properties of recycled concrete, while there has been less discussion of the property prediction model, as based on the electrical resistivity and compressive strength of various concrete materials. Therefore, based on the results of previous studies of concrete with various mixture ratios of waste LCD glass (Wang and Huang 2010a, 2010b), the relationships between the electrical resistivity and the influencing factors, such as waste glass content, water-binder ratio, and age, are chosen as the focus of this study.

2. Characteristics of electrical resistivity and waste LCD glass concrete

Wang *et al*. (2014c) used different ratios by adding LCD glass powder as a replacement for cement, and glass sand as a replacement for natural sand in concrete. The setting time and compressive strength increased as the proportions of the substitute were increased by replacing cement with waste liquid crystal glass in the cement mortar. The compressive strengths of the concrete were decreased when the ratio of glass sand replacement was raised. Moreover, the addition of glass sand provided excellent volume stability. The drying shrinkage values decreased with the increased recycled glass content, which was probably due to the lower water absorption characteristics of glass cullet. Furthermore, glass sand provided higher resistance, and such resistance tended to improve with the increased proportion of concrete, as well as with age. Topcu and Canbaz (2004) reported that the slump, air content, and unit weight of fresh concrete decreased when the proportion of additional waste glass was increased; however, the flow table values increased with the increased addition of waste glass, as waste glass does not absorb water. In addition, the mechanical properties of the concrete, such as the compressive strength, flexural strength, splitting tensile strength, and dynamic modulus of elasticity, decreased as the waste glass content increased, and concrete expansion slowed down when the addition of waste glass content increased. In addition, the results of Ismail and Hashmi (2009), who used recycled glass to partially replace the fine aggregate, and Terro (2006), who used recycled crushed glass with different particle diameters as an aggregate, were observed to follow the same trend as those of Topcu and Canbaz (2004).

Kou and Poon (2009) used recycled-glass sand with a particle diameter of less than 5 mm, a specific gravity of 2.45, and a fineness modulus of 4.25 to study self-consolidating concrete (SCC). The findings indicated that the unit weight and air content decreased when the level of added waste glass increased; however, the decrease in amplitude was small, and the variance in slump flow was slightly influenced by the waste glass content. In addition, expansion slowly increased when the level of added waste glass was increased. The trends of the slump flow and ASR (alkali silica reaction) test results (Kou and Poon 2009) were slightly different from the results of Topcu and Canbaz (2004). Regarding the mechanical properties, the compressive strength, splitting tensile strength, and static elasticity modulus decreased when the waste glass content was increased. Wang (2011) found that, while the slump flow increased with the replacement of glass additive as an aggregate, the compressive strength and flexural strength decreased when the level of added glass was increased. The compressive strength of waste LCD glass concrete also decreased when the replacement of waste glass increased (Lin *et al.* 2012, Park *et al.* 2004, Wang 2009).

Wang and Chen (2010) found that the electrical resistivity of CLSC (controlled low-strength concrete) increased with curing age, and decreased with the increased water-binder ratio; however, electrical resistivity increased with the increasing percentages of the glass-sand substitute. In other words, the lower the water-binder ratio, and the more waste glass is added, the higher the electrical resistance will be. Concrete with lower conductivity and high electrical resistivity provides better protection against corrosion and penetration of harmful substances. While the initial electrical resistivity was very low, it increased markedly with curing age; nevertheless, the electrical resistivity of CLSC mixed with waste glass was relatively low, and the highest resistivity achieved was only 11 kΩ-cm, indicating poor durability.

Electrical resistivity measurements can be used for the performance-based evaluation of concrete material, and is a suitable indicator for concrete penetration and chloride ion permeability. As it is a nondestructive, simple, rapid, and economical method, it can also be used on site. When electrical resistivity is high, the movement of chloride ions in the concrete will be slow, and consequently, the corrosion rate of reinforcements in concrete will decrease (Ramezanianpour *et al.* 2011), therefore, concrete elements will be more durable and have a longer life cycle. The results of Ramezanianpour *et al*.'s (2011) investigation showed that there is a decreasing power relationship between electrical resistivity and water penetration for a wide range of concrete compositions in terms of cement type and water-cement ratio; similarly, rapid chloride penetration has the same tendency. Nevertheless, while there is no sensible correlation between compressive strength and concrete resistivity (R^2=0.413) when concrete mixtures are made with various cementitious materials, the compressive strength will increase with the concrete's resistivity. However, in the case of similar cementitious materials, an increasing linear relationship was observed between the compressive strength and concrete resistivity. Similarly, the results of Ferreira and Jalali (2010) had the same tendency of compressive strength, and a hyperbola equation was proposed for simulating the evolution of electrical resistivity with curing time. Furthermore, most studies show that the electrical resistivity of concrete material increases with curing time through a linear or nonlinear relationship; similarly, compressive strength vs. electrical resistivity has the same tendency (Kahraman

Table 1 Chemical properties of cement, fly ash, slag and LCD glass sand (%) (Wang and Huang 2010a)

Properties	SiO_2	Al_2O_3	Fe_2O_3	CaO	K_2O	Na_2O	SO_3	LoI	S	MgO	TiO_2	P_2O_5
Cement	20.74	4.65	3.10	62.85	-	-	2.36	2.11	-	3.43	-	-
Fly ash	48.26	38.23	4.58	2.84	1.16	0.21	2.36	5.38	-	2.92	1.42	-
Slag	35.47	13.71	0.33	41.00	-	-	0.75	0.95	0.47	6.60	-	-
LCD glass	62.48	16.76	9.41	2.70	1.37	0.64	-	-	-	0.20	0.01	0.01

Table 2 Physical properties of aggregate and glass sand (Wang and Huang 2010a)

Items	Particle density (g/cm^3)	Water absorption (%)	Fineness modulus (F.M.)	D_{max} (mm)	Soil content (%)	Unit weight (kg/m^3)
Coarse aggregate	2.62	0.7	5.02	9.5	0.5	1530
Fine aggregate	2.57	1.2	3.22	1.18	1.3	1820
LCD glass sand	2.45	0.4	3.37	2.36	-	680
Regulatory	ASTM C128	ASTM C128	ASTM C136		ASTM C117	ASTM C29
	ASTM C127	ASTM C127				

Table 3 Glass sand and coarse/fine aggregate sieve analysis (Wang and Huang 2010a)

Mesh (mm)	4.75	2.36	1.18	0.59	0.297	0.149	0.075	Plate
Fine aggregate (%)	99.4	85.3	58.1	32.3	10.2	2.3	0.0	0.0
LCD glass sand (%)	100	99.9	35.6	16.4	8.0	2.7	0.7	0.0
Mesh (mm)	75	50	37.5	25	12.5	9.5	4.75	Plate
Coarse aggregate (%)	100	100	100	100	82.0	54.0	7.0	0.0

Table 4 Mixture proportions of SCGC

w/b	No.	Substation (%)	Binding materials			Aggregate			Unit: kg/m^3	
			Cement	Fly ash	Slag	Coarse aggregate	Sand	Glass sand	Water	SP
0.28	SC28G0	0	463	132	66	786	850	—	185	7.2
	SC28G10	10	463	132	66	786	765	74	185	7.2
	SC28G20	20	463	132	66	786	680	159	185	7.2
	SC28G30	30	463	132	66	786	595	238	185	7.2
0.32	SC32G0	0	405	116	58	786	850	—	185	6.5
	SC32G10	10	405	116	58	786	765	74	185	6.5
	SC32G20	20	405	116	58	786	680	159	185	6.5
	SC32G30	30	405	116	58	786	595	238	185	6.5
0.36	SC36G0	0	360	103	51	786	850	—	185	5.7
	SC36G10	10	360	103	51	786	765	74	185	5.7
	SC36G20	20	360	103	51	786	680	159	185	5.7
	SC36G30	30	360	103	51	786	595	238	185	5.7

and Alber 2014, Liu and Presuel-Moreno 2014, Lubeck *et al.* 2012, Ramezanianpour *et al.* 2014, Xiaosheng *et al.* 2012).

3. Experimental materials and mixtures

A series of tests for self-consolidating glass concrete (SCGC) were performed by Wang and Huang (2010a, 2010b). In this study, slump flow testing is conducted on all the fresh concrete groups according to ASTM C143. The compressive strength, flexural strength, ultrasonic pulse velocity (UPV), and electrical resistivity tests are conducted according to ASTM C39, ASTM C293, ASTM C597, and ASTM C876, respectively. A four-stage resistivity meter (Swiss Proceq Company) is used to measure the electrical resistivity of the specimens. The dimensions of the cylinder for compressive strength, UPV, and electric resistivity testing are 100×200 mm. In addition, 100×100×360 mm cubes are used for flexural strength testing, all the specimens are cast and solidified, the forms are removed after 24 h, and the specimens are placed and cured at room temperature (23-25℃) in saturated limewater. The curing time of specimens is 1, 7, 28, 56, 90, and 180 days for compressive strength, UPV, and electrical resistivity, respectively. Furthermore, the curing time of the specimens is 7, 28, and 90 days for flexural strength. During the tests, the test specimens were saturated surface dry (SSD).

The cement, fly ash, and slag (ground granulated blast furnace slag, GGBFS) used in this study are local materials, which are chosen in compliance with Taiwanese specifications CNS61, CNS3036, and CNS12549, respectively. Particulate waste glass sand, which can pass through a No. 8 sieve, is provided by Chi Mei Optoelectronics. Regarding the waste LCD glasses, the SiO_2 ratio is the highest, at about 62.48%, thus, it acts as a high Si material; also present in the waste LCD glasses, in decreasing order of ratio, are Al_2O_3, Fe_2O_3, CaO, and K_2O. The chemical properties of the cement, fly ash, slag, and glass sand are shown in Table 1. The fineness modulus of the LCD glass sand is 3.37. The physical properties of the aggregate and glass sand are shown in Table 2. The gradations of coarse and fine aggregates to waste glass are shown in Table 3. Based on the reuse of waste materials, the cement is partially replaced by fly ash and slag, while the fine aggregate of natural sand is partially replaced by waste LCD glass. The binder material is mixed with a cement-fly ash-slag ratio of 7:2:1 by weight. The water-to-binder ratios are set as 0.28, 0.32 and 0.36, and 4 types of glass sand are added at volume replacement ratios of 0%, 10%, 20%, and 30%. Fly ash, slag, and superplasticizer are added and blended using a simple SCC (self-consolidating concrete) mixing design method in order to explore the mixing, hardening, and durability properties. The SCGC (self-consolidating glass concrete) mixture proportions are shown in Table 4.

Wang and Huang (2010b) found that the compressive strength of waste LCD glass concrete increased with age; however, the trend became smooth over time and close to a horizontal curve. In addition, the compressive strength of waste LCD glass concrete decreases as the waste glass content increases. The relationship between electrical resistivity and curing time has a tendency similar to compressive strength; nevertheless, electrical resistivity tends to increase with increasing waste glass content. The details of the test results and properties have been described in previous studies (Wang and Huang 2010a, 2010b).

In this study, the results from experiments using various mixture ratios of self-consolidating waste LCD glass

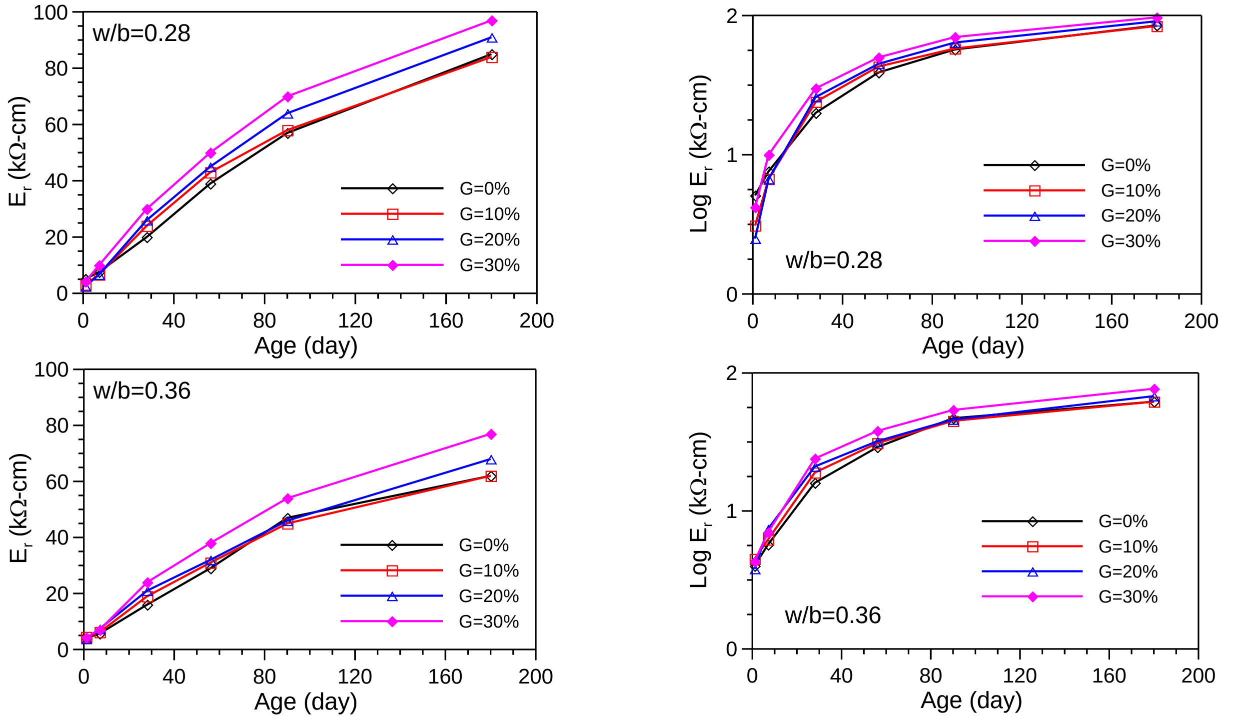

(a) Under normal scale coordinate (b) After transfer to semi-logarithm scale coordinate

Fig. 1 The relationship between electrical resistivity and curing age

Table 5 Values of parameters a_e, b_e, k and ϕ for different mixtures

w/b	Electrical resistivity prediction model			Compressive strength prediction model	
	G	a_e	b_e	k	ϕ
0.28	0	4.901	0.501	7.200	16.462
	0.1	4.733	0.501		
	0.2	4.837	0.490		
	0.3	3.817	0.489		
0.32	0	5.535	0.506	-1.392	17.687
	0.1	4.762	0.506		
	0.2	5.294	0.493		
	0.3	3.886	0.490		
0.36	0	5.515	0.535	-0.609	16.021
	0.1	4.919	0.539		
	0.2	4.805	0.530		
	0.3	4.528	0.513		

concrete form the basis for the discussion of the relationships between the multiple factors influencing electrical resistivity, such as waste glass content, water-binder ratio, and age, in order to establish a predictive analysis model for the evaluation of electrical resistivity. The relationship between compressive strength and electrical resistivity is also established.

4. Studying and planning the prediction model for electrical resistivity and compressive strength

Lubeck *et al.* (2012) used a power increasing function to calculate the relationship between electrical resistivity and curing time, and suggested a linear increasing relation for compressive strength versus electrical resistivity. Liu and Presuel-Moreno (2014) used a hyperbolic equation to evaluate concrete resistivity with curing time, and the 28-day compressive strength showed a nonlinear increase with the increase in electrical resistivity; however, the trend became smooth over concrete resistivity. Nevertheless, the compressive strength for mortar at 28 days could be estimated by electrical resistivity at 24 hours for a sample, and a linear increasing relationship was established (Xiaosheng *et al.* 2012). Furthermore, Ferreira and Jalali (2010) used two approaches for their analysis; first, a hyperbolic equation was proposed for simulating the evolution of electrical resistivity with time for an empirical approach model; second, an exponential function was used to predict the electrical resistivity versus time for a theoretical approach model. In addition, Wang and Chen (2010) employed a mixture design of controlled low-strength concrete, which was mixed using different water-binder ratios and various percentages of sand substituted by waste LCD glass sand, and found that the electrical resistivity increased with the curing age and decreased with the increased water-binder ratio, while the electrical resistivity increased with the increased percentage of the glass-sand substitute.

Based on the characteristics of electrical resistivity and compressive strength, this study considers a number of variables, including the water-binder ratio (w/b), age *t*, and waste glass substitution percentage *G*, in order to deduce the waste LCD glass concrete electrical resistivity and compressive strength prediction models.

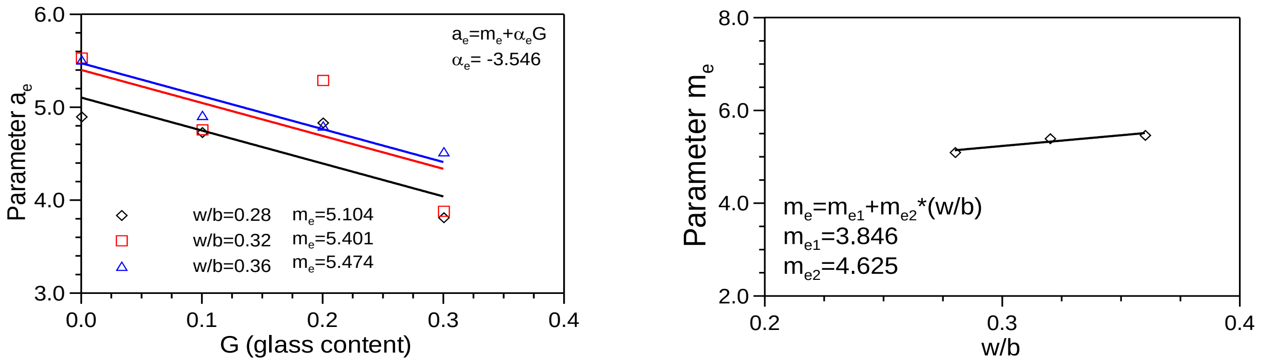

(a) Parameter a_e versus glass content G (b) Parameter m_e versus water-binder ratio (w/b)

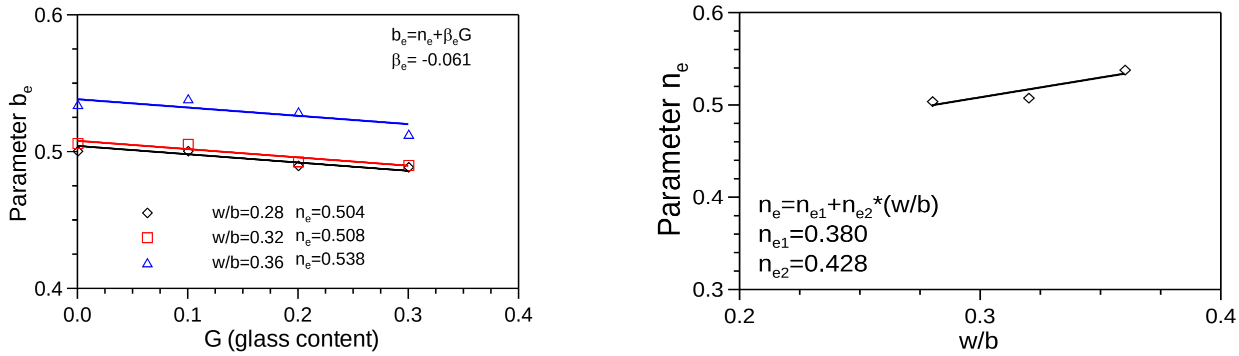

(a) Parameter b_e versus glass content G (b) Parameter n_e versus water-binder ratio (w/b)

Fig. 2 Characteristics of the parameters of the electrical resistivity prediction model

4.1 Development of the electrical resistivity prediction model

The electrical resistivity of waste glass concrete increases with the increased waste glass (Wang and Chen 2010). Therefore, the model in this study assumes that the electrical resistivity of waste glass concrete increases when the waste glass content is increased using an identical mixture ratio.

Fig. 1(a) shows the test results for the electrical resistivity E_r of concrete and different curing ages for different waste glass contents when the water-binder ratios (w/b) are 0.28 and 0.36. Regarding an identical waste glass content G, the electrical resistivity E_r illustrates a slight nonlinear increase with age t; however, the nonlinear relationship is not significant. The electrical resistivity also increases when the waste glass content increases. Fig. 1(b) illustrates that the relationship of electrical resistivity versus age in a semi-logarithm scale coordinate has a significantly nonlinear increase, and the increase becomes smooth as aging increases. In addition, the test results have the same tendency when the water-binder ratio (w/b) is 0.32.

Therefore, the relationship between electrical resistivity and age is simulated using the hyperbolic equation, as shown in Eq. (1), where parameters a_e and b_e (shown in Table 5) are the coefficients of the hyperbolic function, and t is age. When Eq. (1) is transferred back to a normal scale coordinate, it can be rewritten as Eq. (2)

$$y = \log_{10} E_r = f(t) = \frac{t}{a_e + b_e t} \tag{1}$$

$$E_r = \exp\left(2.303 \times \frac{t}{a_e + b_e t}\right) \tag{2}$$

Under identical conditions, parameter a_e increases with the decrease in waste glass content, as based on the test results of electrical resistivity, and increases when the waste glass content increases. Thus, a linear decreasing function between a_e and G is used, which shows that a_e has a parallel relationship to the change in waste glass content, as shown in Fig. 2(a) and Eq. (3). Parameters m_e and a_e are the linear-relationship interception and slope, respectively. Parameters m_e and w/b also exhibit an increasing linear relationship, as shown in Fig. 2(b) and approximated in Eq. (4). Fig. 2(c) shows that parameter b_e also has a linear decreasing relationship with the waste glass content, thus, parameter b_e is expressed, as shown in Eq. (5). Similarly, an increasing linear relationship between parameter n_e and the water-binder ratio (w/b) is shown in Fig. 2(d) and Eq. (6)

$$a_e = f(G) = (m_e + \alpha_e \times G) \tag{3}$$

$$m_e = (m_{e1} + m_{e2}(w/b)) \tag{4}$$

$$b_e = f(G) = (n_e + \beta_e \times G) \tag{5}$$

$$n_e = (n_{e1} + n_{e2}(w/b)) \tag{6}$$

where α_e, β_e, m_e, and n_e are the parameters related to waste glass content G, while m_{e1}, m_{e2}, and n_{e1}, n_{e2} are the

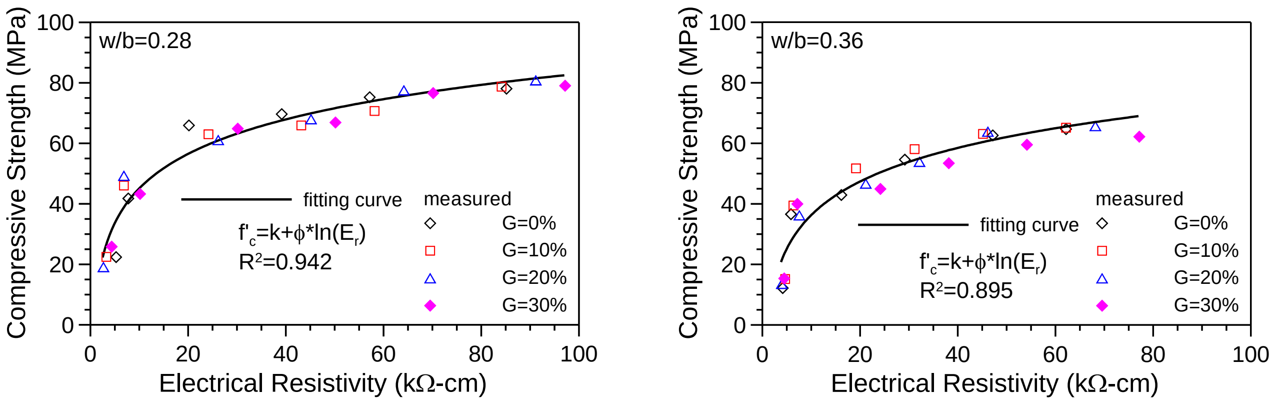

(a) Water-binder ratio w/b is 0.28 (b) Water-binder ratio w/b is 0.36

Fig. 3 The relationship of compressive strength and electrical resistivity with various waste glass contents

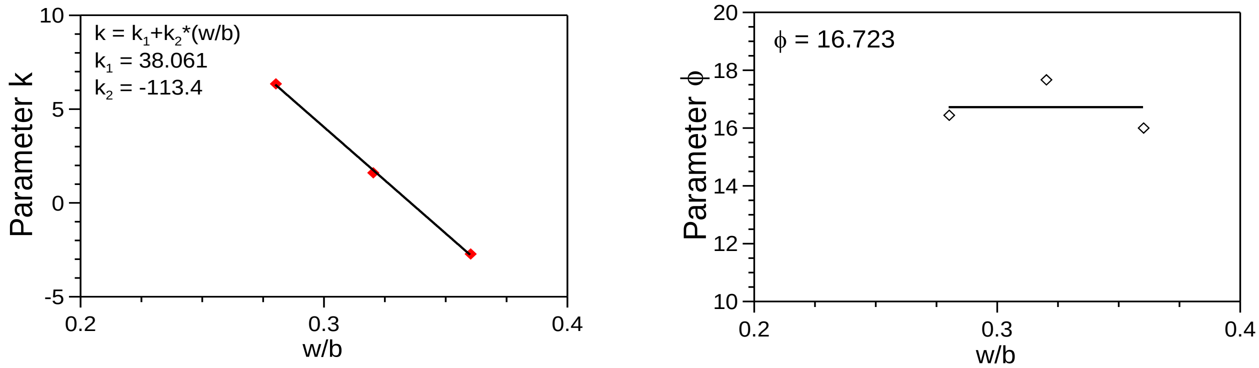

(a) Parameter k versus water-binder ratio (w/b) (b) Parameter ϕ versus water-binder ratio (w/b)

Fig. 4 Characteristics of the parameters of the compressive strength prediction model based on electrical resistivity

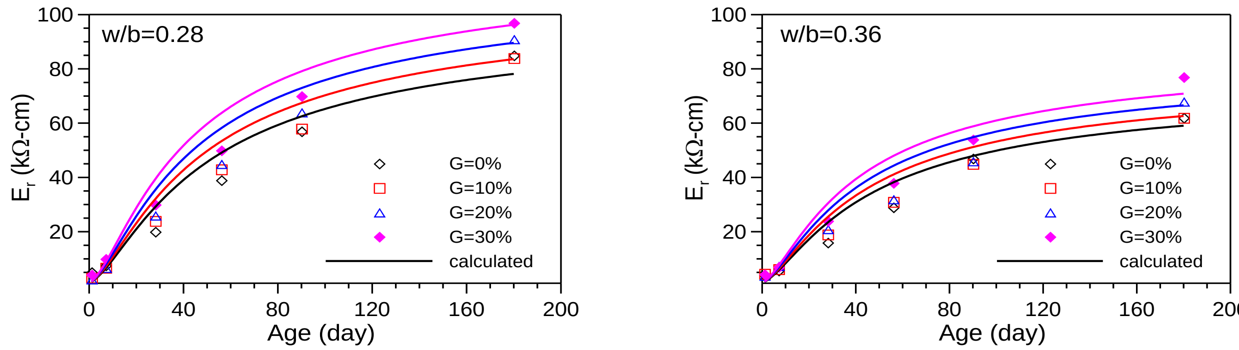

(a) Water-binder ratio (w/b) is 0.28 (b) Water-binder ratio (w/b) is 0.36

Fig. 5 Comparison of predicted model and tested results for electrical resistivity

coefficients related to the water-binder ratio (w/b). Eqs. (3)-(6) are combined, and Eq. (2) can be expressed as Eq. (7). When the prediction model for the electrical resistivity of concrete is used for the model regression analysis of the test results, the model parameters are α_e=−3.546, β_e=−0.061, m_{e1}=3.846, m_{e2}=4.625, n_{e1}=0.380 and n_{e2}=0.428.

$$E_r = \exp\left[2.303\times \frac{t}{[(m_{e1}+m_{e2}(w/b))+\alpha_e\times G]+[(n_{e1}+n_{e2}(w/b))+\beta_e\times G]\times t}\right] \tag{7}$$

4.2 Prediction of compressive strength by electrical resistivity method

Previous researchers have applied the electrical resistivity of concrete to predict compressive strength, and such research often involved the development of the relationship between electrical resistivity and compressive strength. Previous studies have concluded that, for concrete with a particular mix proportion, there was good correlation between electrical resistivity and compressive strength. Nevertheless, the compressive strength of concrete increases with electrical resistivity by a linear or nonlinear relationship (Kahraman and Alber 2014, Liu and Presuel-

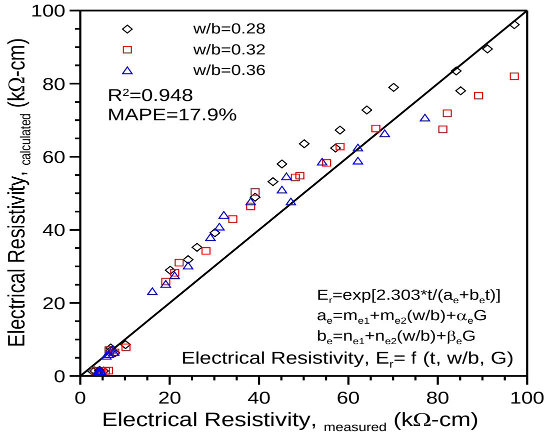

Fig. 6 Comparison of predicted model and tested results for electrical resistivity with different water-binder ratios

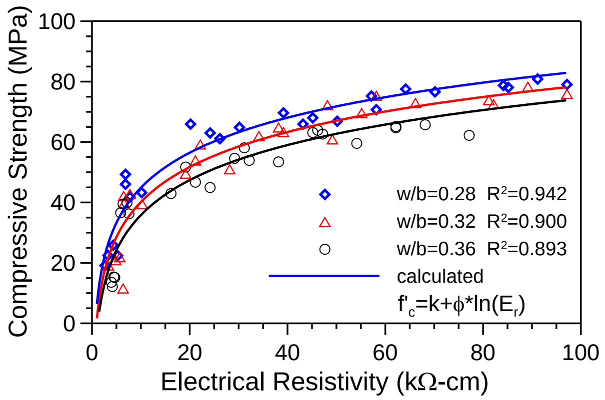

Fig. 7 Comparison of predicted model and tested results for the relationship of compressive strength and electrical resistivity

Moreno 2014, Lubeck *et al.* 2012, Ramezanianpour *et al.* 2014, Xiaosheng *et al.* 2012). Therefore, the relationship of compressive strength versus electrical resistivity may be related to the mix proportions of concrete.

Fig. 3(a) illustrates the test results of the concrete compressive strength and electrical resistivity of different waste glass contents when the water-binder ratio is 0.28. For the same waste glass content G, the compressive strength increases with electrical resistivity E_r, and this increase became smooth using a nonlinear function. However, the change in the relationship between compressive strength and electrical resistivity is not obvious for various waste glass contents. Similar phenomena are observed in other tests with various water-binder ratios, such as those shown in Fig. 3(b). Therefore, the waste glass content effect can be neglected in the procedure for the established prediction model. Thus, the relationship between compressive strength and electrical resistivity is simulated using a logarithm function, as shown in Eq. (8), where parameters k and ϕ (shown in Table 5) are the coefficients of the logarithm function, and E_r is the electrical resistivity of the concrete. Under identical conditions, parameter k decreased with the water-binder ratio, as based on the assumption that the waste glass

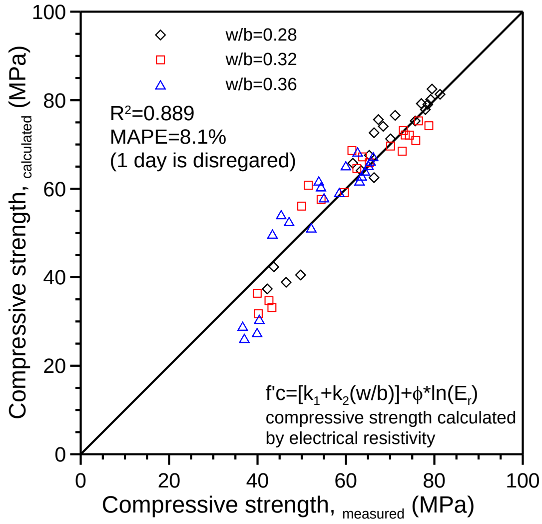

Fig. 8 Comparison of compressive strength with calculations based on electrical resistivity and test results

content effect was not apparent. Thus, parameter k and the water-binder ratio (w/b) exhibit a linear decreasing relationship, as shown in Fig. 4(a) and expressed as Eq. (9). Table 5 shows that parameter ϕ is not affected by the various water-binder ratios; therefore, parameter ϕ is a constant, and is independent of the water-binder ratio, as shown in Fig. 4(b)

$$f_c' = k + \phi \times \ln E_r \tag{8}$$

$$k = k_1 + k_2 \times (w/b) \tag{9}$$

where k and ϕ are the parameters related to electrical resistivity (E_r), while k_1 and k_2 are the coefficients of the water-binder ratio (w/b). Eqs. (7) to (9) are combined, and the compressive strength prediction model is described, as shown in Eq. (10). It is noteworthy that the compressive strength of waste LCD glass concrete can be evaluated by the electrical resistivity of non-destructive testing. When the prediction model of the waste glass concrete compressive strength is applied in the regression analysis of the testing results, the model parameters are k_1=38.061, k_2=−113.40, and ϕ=16.723.

$$f_c' = (k_1 + k_2(w/b)) + \left[2.303 \times \phi \times \frac{t}{[(m_{e1}+m_{e2}(w/b))+\alpha_e \times G]+[(n_{e1}+n_{e2}(w/b))+\beta_e \times G] \times t}\right] \tag{10}$$

5. Comparison between the predictive analysis and the test result

5.1 Electrical resistivity

As shown in Figs. 5(a) and 5(b), the multivariate concrete electrical resistivity prediction model, which considers the water-binder ratio (w/b), age t, and waste glass content G in the previous section, is compared with the test results for water-binder ratios w/b=0.28 and w/b=0.36. As the analysis results suggest, the electrical resistivity prediction model, as based on the hyperbolic model according to the relationship of electrical resistivity versus curing age, is in a semi-logarithm scale coordinate, can accurately evaluate electrical resistivity under different w/b, *t*, and *G* conditions, and the prediction analysis results of other water-binder ratios and waste glass contents suggest the same trends. To validate the accuracy of the prediction model analysis results, this study employs two indices: the MAPE (mean absolute percentage error) (Lewis 1982) value and R^2 (coefficient of determination), in order to determine the error between the model analysis results and the measured value.

The coefficient of determination R^2 is obtained from regression analysis using the model for the predicted electrical resistivity analysis value and the test results. When w/b is 0.28, R^2=0.965; when w/b is 0.32, R^2=0.936, and when w/b is 0.36, R^2=0.950. The analytic results show that when the water-binder ratios (w/b) are 0.28, 0.32, and 0.36, and the test results at the age of one day are disregarded, the MAPE values are 18.2%, 18.4%, and 17.0%, respectively. The comparison of all water-binder ratio analysis values and testing results suggest that the coefficient of determination is R^2=0.948, which is greater than 0.8, and the MAPE=17.9%, which is lower than 20%, as shown in Fig. 6. Lewis (1982) suggested that if the MAPE is less than 10%, the model has excellent predictive ability; if the MAPE is in the range of 10-20%, the model has good predictive ability; and if the MAPE is more than 50%, the prediction results of the model are not accurate. Therefore, the electrical resistivity prediction model, as reported in this paper, has good prediction abilities.

5.2 Compressive strength

As shown in Fig. 7, the compressive strength prediction model (Eq. (10)) is applied in the compressive strength analysis and test results for all waste glass contents and water-binder ratios. The compressive strength prediction model, as based on the electrical resistivity of non-destructive testing, can accurately evaluate compressive strengths at different w/b, *t*, and *G* values. In addition, the coefficient of determination R^2 is obtained from regression analysis, which uses the model (Eq. (10)) for the predicted compressive strength analysis value and the test results: when w/b is 0.28, R^2=0.974; when w/b is 0.32, R^2=0.943; and when w/b is 0.36, R^2=0.941. The analytical results show that when the water-binder ratio (w/b) is 0.28, 0.32, and 0.36, and the test results at the age of one day are disregarded, the MAPE values are 5.9%, 7.7%, and 10.6%, respectively. The comparison of all water-binder ratio analysis values and testing results suggest that the coefficient of determination is R^2=0.889, which is greater than 0.8, and MAPE=8.1%, as shown in Fig. 8.

Wang *et al.* (2014a, 2014b) studied the hardened mechanical properties of waste LCD glass concrete. The compressive strength, flexural strength, and ultrasonic pulse velocity prediction models were also established by the function of waste glass content *G*, water-binder ratio (w/b), and curing age *t*. The compressive strength model is shown as Eqs. (11) and (12); while there is a difference with Eq. (10), they have the same affected factors, such as water-binder ratio, waste glass content, and curing age.

$$\frac{f'_c}{f'_{c,28}} = \frac{t}{[(m_1 + m_2(w/b)) + \alpha \times G] + [(n_1 + n_2(w/b)) + \beta \times G] \times t} \tag{11}$$

$$f'_{c,28} = [x_1 + x_2(w/b)] + \theta \times G \tag{12}$$

The predicted compressive strength analysis values and test results show: when w/b is 0.28, R^2=0.96; when w/b is 0.32, R^2=0.95; and when w/b is 0.36, R^2=0.93. The analytical results show that when the water-binder ratios (w/b) are 0.28, 0.32 and 0.36, and the test results at the age of one day are disregarded, the MAPE values are 5.4%, 7.4%, and 8.4%, respectively. The comparison of all water-binder ratio analysis values and test results suggest that the coefficient of determination is R^2=0.95 and MAPE=7.0%. The predicted results using Eq. (11) are notably similar to the test results. The details of the prediction model and the related parameters are described in the reference (note that the collected model parameters are α=1.48, β=0, m_1=4.30, m_2=2.58, n_1=1.07, n_2=−1.09, θ=−5.10, x_1=124.2 and x_2=−214.3).

Although the compressive strength model based on the electrical resistivity of non-destructive testing, as predicted by Eq. (10), and the results compared with Eq. (11), have a smaller coefficient of determination and a larger MAPE value, the divergence is very small. Therefore, the proposed compressive strength and electrical resistivity analysis models have good prediction capabilities.

6. Conclusions

1. An electrical resistivity of non-destructive testing prediction model is developed in this study, which simultaneously considers multiple variables, including water-binder ratios, waste glass content, and age, and combines the electrical resistivity characteristics of waste glass concrete, as based on the hyperbolic function in a semi-logarithm scale coordinate. The proposed model provides a good reference for the mix proportion designs of adding waste LCD glass to concrete for future engineering applications.

2. Compared with the experimental results, statistical analysis showed that the coefficient of determination R^2 and the MAPE value are in the range of 0.936 to 0.965, and 17.0% to 18.2% for electrical resistivity, respectively. Therefore, the proposed prediction models of electrical resistivity exhibited good predictive capabilities.

3. The prediction analysis results of compressive strength and electrical resistivity were notably similar to the test results, and showed good nonlinear relationship of the logarithm function. Moreover, when the prediction analysis accuracy of compressive strength and electrical resistivity were compared, the MAPE value was 5.9-10.6%, and nearly less than 10%. Therefore, the proposed compressive strength prediction model, as based on electrical resistivity,

has good predictive capabilities. Nevertheless, the characteristics of compressive strength versus electrical resistivity for various water-binder ratios are not affected by the waste glass content in this study. Thus, it should be further studied and validated when the prediction models in this study are applied to other mixing conditions.

References

Breysse, D. (2012), "Nondestructive evaluation of concrete strength: An historical review and a new perspective by combining NDT methods", *Constr. Build. Mater.*, **33**, 139-163.

Chang, H.L. (2005), "An approach to sustainable growth for flat panel display industry in Taiwan", *Sustain. Ind. Devel. Bim.*, **19**, 4-13.

Ferreira, R.M. and Jalali, S. (2010), "NDT measurements for the prediction of 28-day compressive strength", *NDT&E Int.*, **43**(2), 55-61.

Gao, Y.Y., Liu, L.P. and Wang, Y.J. (2008), LCD P*anel Manufacturing Waste Resource Status of Comment*, Green Foundation Newsletters Special Reports.

Ismail, Z.Z. and Hashmi, E.A.A. (2009), "Recycling of waste glass as a partial replacement for fine aggregate in concrete", *Waste Manage.*, **29**(2), 655-659.

Kahraman, S. and Alber, M. (2014), "Electrical impedance spectroscopy measurements to estimate the uniaxial compressive strength of a fault breccia", *Bull. Mater. Sci.*, **37**(6), 1543-1550.

Kou, S.C. and Poon, C.S. (2009), "Properties of self-compacting concrete prepared with recycled glass aggregate", *Cement Concrete Compos.*, **31**, 107-113.

Lewis, C.D. (1982), *Industrial and Business Forecasting Method*, Butterworth Scientific Publishers, London, U.K.

Lin, K.L. (2007), "The effect of heating temperature of thin film transistor-liquid crystal display (TFT-LCD) electric-optical waste glass substitute partial clay as eco-brick", *J. Clean. Prod.*, **15**(18), 1755-1759.

Lin, K.L., Shiu, H.S., Shie, J.L., Cheng, T.W. and Hwang, C.L. (2012), "Effect of composition on characteristics of thin film transistor liquid crystal display (TFT-LCD) waste glass-metakaolin-based geopolymers", *Constr. Build. Mater.*, **36**, 501-507.

Liu, Y. and Presuel-Moreno, F. (2014), "Effect of elevated temperature curing on compressive strength and electrical resistivity of concrete with fly ash and ground-granulated blast-furnace slag", *ACI Mater. J.*, **111**(5), 531-541.

Lubeck, A., Gastaldini, A.L.G., Barin, D.S. and Siqueira, H.C. (2012), "Compressive strength and electrical properties of concrete with white Portland cement and blast-furnace slag", *Cement Concrete Compos.*, **34**(3), 392-399.

Omran, A. and Tagnit-Hamou, A. (2016), "Performance of glass-powder concrete in field applications", *Constr. Build. Mater.*, **109**, 84-95.

Park, S.B., Lee, B.C. and Kim, J.H. (2004), "Studies on mechanical properties of concrete containing waste glass aggregate", *Cement Concrete Res.*, **34**(12), 2181-2189.

Ramezanianpour, A.A., Karein, S.M.M., Vosoughi, P., Pilvar, A., Isapour, S. and Moodi, F. (2014), "Effects of calcined perlite powder as a SCM on the strength and permeability of concrete", *Constr. Build. Mater.*, **66**, 222-228.

Ramezanianpour, A.A., Pilvar, A., Mahdikhani, M. and Moodi, F. (2011), "Practical evaluation of relationship between concrete resistivity, water penetration, rapid chloride penetration and compressive strength", *Constr. Build. Mater.*, **25**(5), 2472-2479.

Roland, M., Werner, B. and Brigitte, S.H. (2004), *Safety of Recovery of LCDs in Compliance with WEEE*, Berlin, Germany.

Sakale, R., Singh, S. and Jain, S. (2016), "Experimental investigation on strength of glass powder replacement by cement in concrete with different dosages", *J. Sci. Technol. Eng.*, **2**(8), 76-86.

Shariq, M., Prasad, J. and Masood, A. (2013), "Studies in ultrasonic pulse velocity of concrete containing GGBFS", *Constr. Build. Mater.*, **40**, 944-950.

Sheilsa, E., O'Connora, A., Schoefsb, F. and Breysse, D. (2012), "Investigation of the effect of the quality of inspection techniques on the optimal inspection interval for structures", *Struct. Infrastruct. Eng.*, **8**(6), 557-568.

Solis-Carcano, R. and Moreno, E. (2008), "Evaluation of concrete made with crushed limestone aggregate based on ultrasonic pulse velocity", *Constr. Build. Mater.*, **22**(6), 1225-1231.

Terro, M.J. (2006), "Properties of concrete made with recycled crushed glass at elevated temperatures", *Build. Environ.*, **41**(5), 633-639.

Topcu, I.B. and Canbaz, M. (2004), "Properties of concrete containing waste glass", *Cement Concrete Res.*, **34**(2), 267-274.

Vipulanandan, C. and Garas, V. (2008), "Electrical resistivity, pulse velocity, and compressive properties of carbon fiber-reinforced cement mortar", *J. Mater. Civil Eng.*, **20**(2), 93-101.

Wang, C.C., Chen, T.T., Wang, H.Y. and Huang, C. (2014a), "A predictive model for compressive strength of waste LCD glass concrete by nonlinear-multivariate regression", *Comput. Concrete*, **13**(4), 531-545.

Wang, C.C., Wang, H.Y. and Huang, C. (2014b), "Predictive models of hardened mechanical properties of waste LCD glass concrete", *Comput. Concrete*, **14**(5), 577-597.

Wang, H.Y. (2009), "A study of the engineering properties of waste LCD glass applied to controlled low strength materials concrete", *Constr. Build. Mater.*, **23**(6), 2127-2131.

Wang, H.Y. (2011), "The effect of the proportion of thin film transistor-liquid crystal display (TFT–LCD) optical waste glass as a partial substitute for cement in cement mortar", *Constr. Build. Mater.*, **25**(2), 791-797.

Wang, H.Y. and Chen, J.S. (2010), "Mix proportions and properties of CLSC made from thin film transition liquid crystal display optical waste glass", *J. Environ. Manage.*, **91**(3), 638-645.

Wang, H.Y. and Huang, W.L. (2010a), "A study on the properties of fresh self-consolidating glass concrete (SCGC)", *Constr. Build. Mater.*, **24**(4), 619-624.

Wang, H.Y. and Huang, W.L. (2010b), "Durability of self-consolidating concrete is using waste LCD glass", *Constr. Build. Mater.*, **24**(6), 1008-1013.

Wang, H.Y., Zeng, H.H. and Wu, J.Y. (2014c), "A study on the macro and micro properties of concrete with LCD glass", *Constr. Build. Mater.*, **50**, 664-670.

Xiaosheng, W., Lianzhen, X. and Zongjin, L. (2012), "Prediction of standard compressive strength of cement by the electrical resistivity measurement", *Constr. Build. Mater.*, **31**, 341-346.

CC